Olefin Epoxidation by Peroxo Complexes of Cr, Mo, and W. A Comparative Density Functional Study

Cristiana Di Valentin,† Philip Gisdakis, Ilya V. Yudanov,‡ and Notker Rösch*

Institut für Physikalische und Theoretische Chemie, Technische Universität München, 85747 Garching, Germany

Received October 26, 1999

The epoxidation of olefins by peroxo complexes of Cr(VI), Mo(VI) and W(VI) was investigated using the B3LYP hybrid density functional method. For the mono- and bisperoxo model complexes with the structures $(NH_3)(L)M(O)_{2-n}(\eta^2\text{-}O_2)_{1+n}$ (n = 0, 1; L = none, NH_3; M = Cr, Mo, W) and ethylene as model olefin, two reaction mechanism were considered, direct oxygen transfer and a two-step insertion into the metal−peroxo bond. The calculations reveal that direct attack of the nucleophilic olefin on an electrophilic peroxo oxygen center via a transition state of spiro structure is preferred as significantly higher activation barriers were calculated for the insertion mechanism than for the direct mechanism. W complexes are the most active in the series investigated with the calculated activation barriers of direct oxygen transfer to ethylene decreasing in the order Cr > Mo > W. Barriers of bisperoxo species are lower than those of the corresponding monoperoxo species. Coordination of a second NH_3 base ligand to the mono-coordinated species, $(NH_3)M(O)_2(\eta^2\text{-}O_2)$ and $(NH_3)MO(\eta^2\text{-}O_2)_2$, results in a significant increase of the activation barrier which deactivates the complex. Finally, based on a molecular orbital analysis, we discuss factors that govern the activity of the metal peroxo group $M(\eta^2\text{-}O_2)$, in particular the role of metal center.

Introduction

Olefin epoxidation is an important reaction in organic synthesis because the produced epoxides are useful intermediates that can be converted to a variety of valuable products.[1] Epoxidation by organic peroxides such as peracids and dioxiranes was extensively studied and found many practical applications.[1] The mechanism of olefin epoxidation by peracids and dioxiranes was studied in detail also using the quantum chemical calculations.[2,3] Recently, epoxidation by transition metal peroxo compounds attracted much attention due to the possibility to control the stereoselectivity and regioselectivity of the reaction via metal ligands of appropriate spatial structure.[4,5]

The peroxo complexes of early transition metals in their highest oxidation states, like Ti(IV), Mo(VI), W(VI), and Re(VII), constitute an important class of compounds active in the epoxidation of olefins.[6−8] Ti(IV) peroxo species are assumed to be an active component in such important catalytic processes as the homogeneous stereoselective Sharpless epoxidation[9] and the heterogeneous epoxidation on Ti silicalites.[10] The bisperoxo complexes $CH_3(L)ReO(O_2)_2$ (L is a base ligand like water or pyridine) are considered as key intermediates in the epoxidation by the recently discovered catalytic system methyltrioxorhenium (MTO)/H_2O_2.[11,12]

Extensive experimental material is available for the peroxo complexes of Cr, Mo, and W.[13] In particular, a number of bisperoxo complexes $(L_1)(L_2)MO(O_2)_2$ (M = Cr, Mo, W) with different combinations of base ligands L_1 and L_2 has been experimentally characterized.[13] The complex $(hmpt)MoO(O_2)_2$ (hmpt = hexamethylphosphoric triamide) was the first to be identified to stoichiometrically epoxidize alkenes in nonpolar solvents,[14] and it became the complex of choice in a number of studies, but complexes with one base ligand are also active.[13] There is evidence that the tungsten analogue, $(hmpt)WO(O_2)_2$, exhibits a higher epoxidation activity.[15] However, no such activity as oxygen transfer agent was reported for

* To whom correspondence should be addressed.

† Permanent address: Dipartimento di Chimica Organica, Università degli Studi di Pavia, V. le Taramelli 10, I-27100 Pavia, Italy.

‡ Permanent address: Boreskov Institute of Catalysis, Siberian Branch of the Russian Academy of Sciences, 630090 Novosibirsk, Russia.

(1) Schwesinger, J. W.; Bauer, T. In *Stereoselective Synthesis;* Helmchen, G., Hoffmann R. W., Mulzer J., Schaumann E., Eds.; Houben Weyl Thieme: New York, 1995; Vol. E21e, p 4599−4648.

(2) (a) Yamabe, S.; Kondou, C.; Minato, T. *J. Org. Chem.* **1996**, *61*, 616−620. (b) Bach, R. D.; Glukhovtsev, M. N.; Gonzalez, C.; Marquez, M.; Estevez, C. M.; Babul, A. G.; Schlegel, H. B. *J. Phys. Chem. A* **1997**, *101*, 6092−6100. (c) Singleton, D. A.; Merrigan, S. R.; Liu, J.; Houk, K. N. *J. Am. Chem. Soc.* **1997**, *119*, 3385−3386. (d) Bach, R. D.; Glukhovtsev, M. N.; Gonzalez, C. *J. Am. Chem. Soc.* **1998**, *120*, 9902−9910. (e) Freccero, M.; Gandolfi, R.; Sarzi, M.; Rastelli, A. *J. Org. Chem.* **1999**, *64*, 3853−3860.

(3) (a) Houk, K. N.; Liu, J.; DeMello, N.; Condroski, K. R. *J. Am. Chem. Soc.* **1997**, *119*, 10147−10152. (b) Liu, J.; Houk, K. N.; Dinoi, A.; Fusco, C.; Curci, R. *J. Org. Chem.* **1998**, *63*, 8565−8569. (c) Freccero, M.; Gandolfi, R.; Sarzi, M.; Rastelli, A. *Tetrahedron* **1998**, *54*, 6123−6134.

(4) Sheldon, R. A. *Catalytic Oxidation with Hydrogen Peroxide as Oxidant*; Kluwer Academic Publishers: Rotterdam, 1992.

(5) Finn, M. G.; Sharpless, K. B. In *Asymmetric Synthesis*; Morrison, J. D., Ed.; Academic Press: New York, 1986, Vol. 5, pp 247−308.

(6) Mimoun, H. In *Chemistry of Peroxides*; Patai, S., Ed.; Wiley: Chichester, 1983; p 463−520.

(7) Jørgensen, K. A. *Chem. Rev.* **1989**, *89*, 431−458.

(8) Romão, C. C.; Kühn, F. E.; Herrmann, W. A. *Chem. Rev.* **1997**, *97*, 3197−3246.

(9) (a) Sharpless, K. B.; Verhoeven, T. R. *Aldirichim. Acta* **1979**, *12*, 63−73. (b) Johnson, R. A.; Sharpless, K. B. In *Comprehensive Organic Synthesis*; Trost, B. M., Ed.; Pergamon Press: New York, 1991; Vol. 7, Chapter 3.2, p 389−436.

(10) Clerici, M. G.; Ingallina, P. *J. Catal.* **1993**, *140*, 71−83.

(11) Herrmann, W. A.; Fischer, R. W.; Marz, D. W. *Angew. Chem., Int. Ed. Engl.* **1991**, *30*, 1641.

(12) Gisdakis, P.; Antonczak, S.; Köstlmeier, S.; Herrmann, W. A.; Rösch, N. *Angew. Chem., Int. Ed. Engl.* **1998**, *37*, 2211−2214.

(13) Dickman, M. H.; Pope, M. T. *Chem. Rev.* **1994**, *94*, 569−584.

(14) Mimoun, H.; De Roch, I. S.; Sajus, L. *Tetrahedron* **1970**, *26*, 37−50.

10.1021/jo9916784 CCC: $19.00
Published on Web 04/20/2000

analogous Cr peroxo compounds,[13] while Cr oxo complexes can easily undergo epoxidation reactions.[16] As for oxo compounds of other late first-row transition metals, oxygen transfer from the oxo-metal bond to an alkene is observed, but at present it remains open whether this reaction follows a concerted, ionic or diradical mechanism.[7,17] The epoxidation activity of the complexes $(L)MO(O_2)_2$ (M = Mo, W) is inhibited by strongly coordinating solvents.[14,15] This finding led to an extensive discussion of the reaction mechanism.[6,7,14,15,18−21] Initially, it was proposed[14] that the olefin substrate first binds to the metal center and then inserts into a metal-peroxo bond forming a five-membered metallacycle intermediate which in turn decomposes into the epoxide and an oxo complex. In this model the inhibiting effect was interpreted to result from a solvent molecule which occupies a free coordination position at the metal center. However, later investigations favored a mechanism which involves the direct attack of the substrate on a peroxo oxygen center.[12,15,18,21] In that case the solvent effect was attributed to the reduced electrophilicity of the peroxo group due to induction of electron density from the additional solvent ligand via the metal center. Currently, there is considerable interest in the synthesis of new Mo and W complexes for the epoxidation of olefins. In particular, recently it was shown that seven-coordinated bisperoxo complexes $(L1\text{-}L2)MoO(O_2)_2$ with bidentate L1−L2 base ligands are able to catalyze epoxidation by *tert*-butyl hydroperoxide as oxidant, and the formation of a MoOOt-Bu group as active center was proposed.[22]

Quantum chemical calculations using density functional (DF) methods for determining the electronic structure provide valuable information on olefin epoxidation by transition metal peroxo complexes, e.g., on structures of reactive intermediates and transition states, on activation barriers for conceivable competitive pathways of oxygen transfer and on the reaction mechanism including reaction energetics.[12,23−25] DF investigations combined with experimental studies[12,24] were able to shed light onto the MTO catalyzed epoxidation. A recent computational study on model peroxo complexes revealed the significantly higher epoxidation activity of TiOOH species compared to Ti(η^2-O_2) compounds.[25,26]

In contrast to the peroxo complexes of Re and Ti there are only few theoretical studies on group VI peroxo complexes, and those available are only at a semiempirical level. The extended Hückel theory (EHT) was applied to study the decomposition of the five-membered metallacycle intermediate proposed by Mimoun for the epoxidation by Mo bisperoxo complexes.[27] Another EHT study proposed the coordination of ethylene to the Mo center of an $MoO(O_2)_2$ complex as the first step followed by a slipping motion of ethylene toward one of the peroxygens and the formation of a three-membered transition state rather than the five-membered metallacycle intermediate.[28] Using an NDDO approach, the electrophilic properties of six- and seven-coordinated diperoxo species of Mo were compared via calculated electron affinities.[29] Although a higher electron affinity was computed for the six-coordinated species favoring a mechanism that involves a direct nucleophilic attack, no detailed information on the reaction mechanism was presented.

The very close similarity between peroxo species of the group VI elements Mo and W with the group VII analogous Re offers a chance to unravel some fundamental aspects of the epoxidation reaction catalyzed by peroxo complexes of transition metals. The goals of the present computational study are: (i) to investigate the mechanism of olefin (ethylene) epoxidation by peroxo complexes of Cr, Mo, and W (placing special emphasis on a comparison of the direct olefin attack of the peroxo group with the two-step insertion mechanism); (ii) to identify factors that govern the reactivity of metal peroxo groups, among them the specific role of the metal center in the activation/deactivation of the peroxo group; and (iii) to study the effect of additional base ligands of the metal center on the activity of peroxo complex.

Computational Details

We carried out density functional (DF) calculations[30] employing the hybrid B3LYP scheme to describe the exchange-correlation contribution to the electron−electron interaction.[31] LANL2 effective core potentials were used to replace the core electrons of Cr, Mo and W (except for the outermost shells).[32] The corresponding basis sets[32] for the valence and the outermost core electrons of the transition elements were used in the contraction (441/2111/*n*1), where $n = 4$, 3, 2 for Cr, Mo, W, respectively. For main group elements we employed rather flexible 6-311G(d,p) basis sets.[33] All geometry optimizations of intermediates and transition states were performed without any symmetry constraints. The transition state structures

(15) Amato, G.; Arcoria, A.; Ballistreri, F. P.; Tomaselli, G. A.; Bortolini, O.; Conte, V.; Di Furia, F.; Modena, G.; Valle, G. *J. Mol. Cat.* **1986**, *37*, 165−175. Mimoun, H. *Angew. Chem., Int. Ed. Engl.* **1982**, *21*, 734−750.

(16) Paquette, L. A.; Kobayashi, T. *Tetrahedron Lett.* **1987**, *28*, 3531−3534.

(17) (a) Imanishi, H.; Katsuki, T. *Tetrahedron Lett.* **1997**, *38*, 251−254. (b) Fujii, H.; Yoshimura, T.; Kamado, H. *Inorg. Chem.* **1997**, *36*, 1122−1127. (c) Linker, T. *Angew. Chem., Int. Ed. Engl.* **1997**, *36*, 2060−2062. (d) Palucki, M.; Finney, N. S.; Pospisil, P. J.; Güler, M. L.; Ishida, T.; Jacobsen, E. N. *J. Am. Chem. Soc.* **1998**, *120*, 948−954 and references therein.

(18) Sharpless, K. B.; Townsend, J. M.; Willians, I. D. *J. Am. Chem. Soc.* **1972**, *94*, 295−296.

(19) Mimoun, H. *Angew. Chem., Int. Ed. Engl.* **1982**, *21*, 734−750.

(20) Camprestini, S.; Di Furia, F.; Modena, G.; Bortolini, O. *J. Org. Chem.* **1988**, *53*, 5721−5724.

(21) Talsi, E. P.; Shalyaev, K. V.; Zamaraev, K. I. *J. Mol. Catal.* **1993**, *83*, 347−366.

(22) (a) Thiel, W. R.; Priermeier, T. *Angew. Chem., Int. Ed. Engl.* **1995**, *34*, 1737−1738. (b) Thiel, W. R.; Eppinger J. *Chem. Eur. J.* **1997**, *3*, 696−705. (c) Thiel, W. R. *J. Mol. Catal. A* **1997**, *117*, 449−454.

(23) Görling, A.; Trickey, S. B.; Gisdakis, P.; Rösch N. In *Topics in Organometallic Chemistry*; Brown, J., Hofmann, P., Eds.; Springer: Heidelberg, 1999; Vol. 4, pp 109−163.

(24) Kühn, F. E.; Santos, A. M.; Roesky, P. W.; Herdtweck, E.; Scherer, W.; Gisdakis, P.; Yudanov, I. V.; Di Valentin, C.; Rösch, N. *Chem. Eur. J.* **1999**, *5*, 3603−3615.

(25) Yudanov, I. V.; Gisdakis, P.; Di Valentin, C.; Rösch, N. *Eur. J. Inorg. Chem.* **1999**, 2135−2145.

(26) (a) Wu, Y.-D.; Lai, D. K. W. *J. Am. Chem. Soc.* **1995**, *117*, 11327−11336. (b) Wu, Y.-D.; Lai, D. K. W. *J. Org. Chem.* **1995**, *60*, 673−680.

(27) (a) Purcell, K. F. *J. Organomet. Chem.* **1983**, *252*, 181−185. (b) Purcell, K. F. *Organometallics* **1985**, *4*, 509−514.

(28) Jørgensen, K. A.; Hoffmann, R. *Acta Chem. Scand. B* **1986**, *40*, 411−419.

(29) Filatov, M. J.; Shalyaev, K. V.; Talsi, E. P. *J. Mol. Catal.* **1994**, *87*, L5−L9.

(30) Gaussian 94, Revision D.4: Frisch, M. J.; Trucks, G. W.; Schlegel, H. B.; Gill, P. M. W.; Johnson, B. G.; Robb, M. A.; Cheeseman, J. R.; Keith, T.; Petersson, G. A.; Montgomery, J. A.; Raghavachari, K.; Al-Laham, M. A.; Zakrzewski, V. G.; Ortiz, J. V.; Foresman, J. B.; Cioslowski, J.; Stefanov, B. B.; Nanayakkara, A.; Challacombe, M.; Peng, C. Y.; Ayala, P. Y.; Chen, W.; Wong, M. W.; Andres, J. L.; Replogle, E. S.; Gomperts, R.; Martin, R. L., Fox, D. J.; Binkley, J. S.; Defrees, D. J.; Baker, J.; Stewart, J. P.; Head-Gordon, M.; Gonzalez, C.; Pople J. A. Gaussian, Inc., Pittsburgh, PA, 1995.

(31) (a) Becke, A. D. *J. Chem. Phys.* **1993**, *98*, 5648−5651. (b) Lee, C.; Yang, W.; Parr, R. G. *Phys. Rev. B* **1988**, *37*, 785−789.

(32) Hay, P. J.; Wadt, W. R. *J. Chem. Phys.* **1985**, *82*, 299−310.

(33) Krishnan, R.; Binkley, J.; Seeger, R.; Pople, J. *J. Chem. Phys.* **1980**, *72*, 650−654.

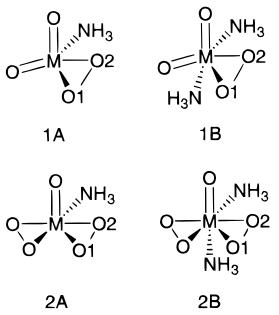

Figure 1. Model complexes of Cr, Mo, and W.

were searched by numerically estimating the matrix of the second-order energy derivatives at every optimization step and by requiring exactly one eigenvalue of this matrix to be negative. Reaction energies and activation barriers were evaluated in single-point fashion with the Cr, Mo, and W basis sets augmented by f-orbital polarization exponents (1.8051 and 0.4966 for Cr, 0.79063 and 0.27345 for Mo, 0.7287 and 0.2425 for W).[34] The natural bond orbital approach[35] (NBO) was used to analyze atomic charges and chemical bonds.

Results

Model Complexes. The dioxo-monoperoxo (**1**) and oxo-bisperoxo (**2**) model complexes employed are shown in Figure 1. For each peroxo type, two types of metal ligand spheres were considered, with one (**A**) and two (**B**) NH_3 base ligands. The metal center was varied along the series Cr, Mo, and W. The bisperoxo dicoordinated species **2B** is seven-coordinated if one takes the total coordination of the metal center into account; it can be related to a number of the experimentally characterized complexes $(L1)(L2)MO(O_2)_2$ (M = Cr, Mo, W) where L1 and L2 correspond either to two monodentate base ligands or to one bidentate ligand.[13] NH_3 is used to model monodentate ligands since we intend to focus on electronic effects of base ligands on the properties of the metal peroxo groups; we shall refrain from studying steric effects. Bidentate ligands that are stable in oxidative conditions bear two nitrogen donor centers as part of an aromatic ring system, like 2,2′-bipyridine or pyrazolylpyridine; such ligands are often used to provide coordinative stability to Mo bisperoxo complexes and to make them soluble in organic solvents.[22] From our computational study of bisperoxo complexes of Re[24] where we considered various base ligands (among them NH_3 and pyridine), we are confident that ammonia provides an adequate model for the electronic influence of more complicate nitrogen-containing base ligands.

All experimentally characterized bisperoxo complexes of Cr, Mo, and W exhibit a pentagonal bipyramidal structure with a seven-coordinated metal center,[13] except for the six-coordinated pentagonal pyramidal complex $(py)CrO(O_2)_2$.[36] Nevertheless, low coordinated species, corresponding to our model **2A**, are supposed to be the most active intermediates in oxygen transfer reactions of Mo and W complexes.[20,21] The calculated structures of the models **2A** exhibit a pentagonal pyramidal shape where the NH_3 ligand occupies the energetically more favorable equatorial position. The models **2A** of Mo and W can be easily transformed into the thermodynamically more stable complex **2B**; the energies of NH_3 addition are −14.9 and −18.2 kcal/mol for Mo and W, respectively. For Cr we were unable to obtain a stable **2B**-type structure.

Although there are no experimental structures available that correspond to the monoperoxo species **1A** and **1B**, related complexes should occur as a result of the oxygen transfer from bisperoxo species of the types **2A** and **2B** to a nucleophilic substrate, i.e., an olefin. As in the case of the bisperoxo models we are able to optimize only the mono-coordinated species **1A** for Cr. For Mo and W, the binding energies of a second ammonia ligand to **1A** are −26.2 and −28.8 kcal/mol, respectively. The trans conformation of two NH_3 ligands shown in Figure 1 exhibits the lowest energy for the models **1B** of Mo and W. The cis conformation of the NH_3 ligands (determined to be the most stable structure of the models **2B**) was found to represent a local minimum of complex W **1B** that lies 19.0 kcal/mol higher in energy; therefore, we will refrain from discussing it in the following.

The calculated geometries of the model complexes can be compared to the results of X-ray analyses which are available for the bisperoxo complexes of Cr, Mo, and W.[36−38] Suitable examples for comparison are complexes of Cr[37] and Mo[38] with bidentate bipyridine ligands, and of Cr with pyridine at the equatorial position.[36] Since no X-ray structure of a W bisperoxo derivative with amino ligands seems to be available, we compare to the complex $(hmpt)(H_2O)WO(O_2)_2$[15] (with hmpt in equatorial position). In Table 1 we compare pertinent calculated geometry parameters to experimental structures. The metal−base distances r(M−N) calculated for the model complexes notably overestimate the corresponding experimental data. This finding is similar to that of the $Re-OH_2$ distance in a bisperoxo complex.[12,39] Best agreement is obtained when the calculated structures Cr **2A** and Mo **2B** are compared with experimental complexes of pyridine[36] and bipyridine base ligands,[38] respectively. The distance from the Mo center to the equatorial nitrogen center is calculated too long by 0.06 Å, and that to the axial nitrogen center is too long by 0.26 Å. Thus, the ligand binding is inferred to be significantly weaker at the axial than at the equatorial position. The corresponding part of the potential energy surfaces is rather flat so that small perturbations may cause rather large structural effects. In any case, common exchange-correlation functionals are known to be less accurate for weak interactions.[23] Recently the binding of different base ligands L to a metal center of a peroxo complex was studied for the structurally similar complexes $H_3C(L)$-$ReO(O_2)_2$.[24] The Re−N distance for the ligand pyridine in the axial position was calculated by 0.07 Å longer than for the ligand NH_3; it corresponds to a binding energy that is smaller by about 2 kcal/mol.[24]

The agreement between the calculated geometry of the model W **2B** and the experimental structures of the complex $(hmpt)(H_2O)WO(O_2)_2$ is less satisfactory.[15] Crucial structural characteristics are the distances O−O

(34) The exponents were determined as described previously for Re; see ref 12 and: Gisdakis, P.; Antonczak, S.; Rösch, N. *Organometallics* **1999**, *18*, 5044−5056.

(35) Reed, A. E.; Curtiss, L. A.; Weinhold, F. *Chem. Rev*. **1988**, *88*, 899−926.

(36) Stomberg, R. *Ark. Kemi* **1964**, *22*, 29−47.

(37) Stomberg, R.; Ainalem, I.-B. *Acta Chem. Scand.* **1968**, *22*, 1439−1451.

(38) Schlemper, E. O.; Schrauzer, G. N.; Hughes, L. A. *Polyhedron* **1984**, *3*, 377−380.

(39) Herrmann, W. A.; Fischer, R. W.; Scherer, W.; Rauch, M. U. *Angew. Chem., Int. Ed. Engl.* **1993**, *32*, 1157−1160.

Table 1. Comparison of Calculated Structures of Various Bisperoxo Complexes with Available Experimental X-ray Crystal Data (All Values in Å)

	r(O−O)[a]	r(M−O_{per})[b]	r(M═O_{oxo})[c]	r(M−L_{eq})[d]	r(M−L_{ax})[d]
$CrO(O_2)_2(NH_3)$, **2A** calcd	1.40	1.82	1.55	2.11	-
$CrO(O_2)_2$py, expt[e]	1.40	1.81	1.58	2.05	-
$MoO(O_2)_2(NH_3)_2$, **2B** calcd	1.44	1.97	1.70	2.26	2.57
$MoO(O_2)_2$bipy, expt[f]	1.46	1.93	1.68	2.20	2.31
$MoO(O_2)_2$(hmpt)(H_2O), expt[g]	1.50	1.94	1.66	2.06	2.35
$WO(O_2)_2(NH_3)_2$, **2B** calcd	1.47	1.96	1.72	2.24	2.51
$WO(O_2)_2$(hmpt)(H_2O), expt[h]	1.52	1.95	1.62	2.06	2.32

[a] Bond length of peroxo group. [b] Distance from the metal center to a peroxo oxygen center, averaged over r(M−O1) and r(M−O2); see Figure 1. [c] Distance from the metal center to the oxo center. [d] Distances from the metal center to the base nitrogen centers in equatorial (eq) and axial (ax) positions (see Figure 1). [e] Reference 36. [f] Reference 38. [g] Reference 40. [h] Reference 15.

Table 2. Calculated Properties of Various Tungsten Model Peroxo Complexes and of the Corresponding Ethylene Epoxidation Front Spiro Transition States (Back Spiro in Parentheses)[a]

	1A	**1B**	**2A**	**2B**
geometry of complex, Å				
r(M−O1)	1.93	1.97	1.95	1.96
r(M−O2)	1.98	1.97	1.94	1.97
r(O1−O2)	1.48	1.46	1.48	1.47
r(M−N_{eq})	2.20	2.27	2.23	2.24
r(M−N_{ax})		2.27		2.51
NBO atomic charges, e				
q(W)	2.30	2.15	2.24	2.24
q(O1)	−0.46	−0.49	−0.44	−0.46
q(O2)	−0.53	−0.49	−0.50	−0.50
geometry of transition states, Å				
r(M−O1)	1.97 (1.83)	2.10	2.00 (1.84)	2.02 (1.73)
r(M−O2)	1.88 (2.08)	1.86	1.86 (2.08)	1.87 (2.08)
r(O1−O2)	1.89 (1.89)	1.87	1.82 (1.85)	1.88 (1.86)
r(O1−C1)	2.16 (2.00)	1.81	2.12 (2.28)	2.11 (2.29)
r(O1−C2)	2.16 (2.12)	2.17	2.24 (1.86)	2.07 (1.80)
r(C1−C2)	1.35 (1.36)	1.37	1.35 (1.37)	1.36 (1.38)

[a] Bond distances r and NBO atomic charges q for the designation of structures; see Figure 1.

(1.47 Å calcd; 1.53 Å expt), W═O_{oxo} (1.72 Å calcd; 1.62 Å expt), and W−L_{eq} (2.24 Å calcd; 1.93 Å expt).[15] However, at least in part, these discrepancies can be attributed to the different sets of base ligands in the complex (hmpt)(H_2O)$WO(O_2)_2$ and the computational model. This can be deduced from the fact that the experimental structure of the analogous molybdenum complex (hmpt)(H_2O)$MoO(O_2)_2$[40] differs only slightly from the structure of its tungsten congener, but exhibits similar deviations from the calculated geometry of the model **2B** Mo (Table 1). In summary, the present models perform satisfactorily for peroxo complexes with amino ligands, but are less accurate for complexes with oxygen containing ligands, such as H_2O and hmpt.

To analyze the calculated properties of different models shown in Figure 1 in more detail we consider the special case of W for which a complete set of models is available (Table 2). Note that the trends obtained for W are also valid for the corresponding series of Cr and Mo. As an example of the changes brought by the variation of metal center we compare in Table 3 the monocoordinated bisperoxo model complexes **2A** of Cr, Mo, and W.

Table 2 presents pertinent structural parameters of the models **1A**, **1B**, **2A**, and **2B** of W and the corresponding results of the NBO population analysis. Species **1A** is characterized by a mirror plane which passes through the centers W, O1, O2, and N (Figure 1). The oxygen centers of peroxo group are not equivalent (even in the absence of the NH_3 ligand) as can be seen from the distances W−O1, 1.93 Å and W−O2, 1.98 Å (Table 2).

Table 3. Calculated Characteristics of Metal Peroxo Groups in Monocoordinated Bisperoxo Complexes 2A (Figure 1) of Cr, Mo, and W[a]

	Cr	Mo	W
geometry of the metal peroxo groups, Å			
r(M−O1)	1.85	1.97	1.95
r(M−O2)	1.80	1.94	1.94
r(O1−O2)	1.40	1.45	1.48
NBO atomic charges, e			
q(M)	0.93	1.96	2.24
q(O1)	−0.23	−0.38	−0.44
q(O2)	−0.26	−0.43	−0.50
NBO analysis of M−O bonds			
n_{M-O1}, e	1.79	1.82	1.86
n_{M-O1}(M)/n_{M-O1}	0.26	0.17	0.15
n_{M-O2}, e	1.79	1.85	1.88
n_{M-O2}(M)/n_{M-O2}	0.25	0.17	0.15
geometry of transition state, Å			
r(M−O1)	1.93	2.02	2.00
r(M−O2)	1.70	1.71	1.86
r(O1−O2)	1.75	1.80	1.82
r(O1−C1)	2.12	2.08	2.12
r(O1−C2)	2.11	2.21	2.24
r(C1−C2)	1.36	1.36	1.35

[a] Bond distances r, NBO atomic charges q, NBO occupations n_{M-O} of M−O bonds and metal contribution n_{M-O}(M)/n_{M-O} to the M−O bond; geometry parameters of the corresponding ethylene epoxidation front spiro transition states.

On the other hand, these metal−oxygen distances hardly change along the series of model complexes (Table 2). This holds also for the geometry of the peroxo groups: the O−O bond lengths range from 1.46 to 1.48 Å (Table 2). Model complex **1B** is the only one in present study that exhibits a symmetric peroxo group with equivalent oxygen centers. In model **2A** the plane defined by the

(40) Le Carpentier, P. J.-M.; Schlupp, R.; Weiss, R. *Acta Crystallogr. B*. **1972**, *28*, 1278−1288.

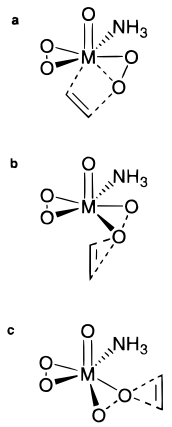

Figure 2. Schematic representation of the transition state structures of the various mechanisms of olefin epoxidation studied: (a) insertion, (b) front spiro, (c) back spiro.

metal center, the oxo ligand and the nitrogen center is a symmetry plane which is preserved even after addition of the second ammonia ligand in complex **2B**. The asymmetry of the peroxo groups in **1A**, **2A**, and **2B** is also reflected by the charge distribution: the oxygen center O1 always carries a smaller negative charge than center O2 which is located closer to the equatorial base ligand. Inspection of the geometry of complex **2A** for different metal centers shows (see Table 3) that significant changes occur in the geometry of metal peroxo group when the metal center is varied. The M−O distance of the Cr complex is by about 0.1 Å shorter than in corresponding Mo and W species, consistent with the smaller ionic radius of Cr(VI). The O−O distance in this series increases from 1.40 Å for Cr to 1.45 Å for Mo and 1.48 Å for W. This calculated trend is in line with the X-ray structures discussed above as well as with IR spectroscopy data which indicate a general decrease of the O−O stretching frequency in the peroxo complexes of the series Cr, Mo, W.[41] Thus, the geometry of the metal peroxo group depends strongly on the metal center of the complex. The influence of the coordination shell can be considered as a second-order effect: as shown above for the W species, the structure of the metal peroxo group undergoes minor changes only in different model complexes with the same metal center.

Ethylene Epoxidation Transition States. To study the epoxidation activity of the various intermediates described above, we determined in each case transition states of oxygen transfer reactions to the model olefin ethylene. The activation barriers were calculated with respect to the energies of the corresponding "free" complexes and an ethylene molecule. As mentioned above, we considered those two mechanisms which are most often discussed in the literature for epoxidation by transition metal peroxo complexes: the insertion mechanism[6,7,14,19] first proposed by Mimoun and a direct attack of the olefin on the peroxo group as suggested by Sharpless and others.[15,18,20,21] For the first mechanism we calculated the transition states for insertion of an ethylene molecule into the peroxo-metal bond (Figure 2) which leads to a metallacycle intermediate. Since the insertion mechanism assumes the availability of a free coordination at the metal center for the precoordination of the olefin this mechanism was considered only for the low-coordinated species **1A** and **2A**. Also, for these complexes we found significantly lower barriers for the direct attack than for the insertion (see below); therefore, we refrained from a more detailed study of this mechanism and did not calculate the barriers for extrusion of the epoxide from the metallacycle.

Table 4. Activation Barriers (in kcal/mol) Calculated for Various Mechanisms of Ethylene Epoxidation by Model Peroxo Complexes of Cr, Mo, and W[a]

		Cr	Mo	W
front spiro				
	1A	22.8	18.8	13.7
	1B	40.1	34.1	31.5
	2A	19.3	14.1	10.7
	2B	*b*	19.7	16.9
back spiro				
	1A	28.9	22.8	19.8
	2A	34.5	28.9	25.9
	2B	*b*	27.5	24.2
insertion				
	1A	28.1	26.4	20.5
	2A	27.3	22.3	18.2

[a] For the designation of the structures, see Figure 1. [b] One NH_3 ligand is expelled during the geometry search; thus, no intermediate of this type could be localized.

For the direct mechanism the attack of both "front" and "back" peroxo oxygen centers was considered.[12] By "front" and "back" we refer to the oxygen centers O1 and O2, respectively, i.e., distant from or close to the equatorial NH_3 ligand (Figure 1). All transition structures of the direct attack exhibit a spiro orientation of ethylene unit where the olefin C−C bond is almost orthogonal to the plane formed by the peroxo group and the metal center. Early theoretical studies of the epoxidation by peroxo complexes of Ti[23] and organic peracids[2] had shown that transition state structures with a coplanar orientation of ethylene (imposed as symmetry constraint) resulted in higher barriers than the corresponding spiro structures. In the present work no planar transition structures were identified since the localization of the transition structure without symmetry constraints always converged to the spiro orientation, independent of the initial geometry. We confirmed the nature of all located spiro and insertion transition states as first-order saddle points on the corresponding potential energy hypersurfaces by a full vibrational analysis; each of these structures was found to exhibit a single imaginary frequency.

The resulting activation barriers calculated for direct front and back spiro attacks as well as for insertion are collected in Table 4. For all considered species the direct attack of the peroxo front-oxygen center yields the lowest activation barriers. Much higher activation barriers are obtained for attack from the "back" for species with a nonsymmetric peroxo group, namely for **1A**, **2A**, and **2B**. For the low coordinated species **1A** and **2A** the insertion mechanism also yields high activation barriers; for the complexes **1A** of Mo and W these barriers are even higher than those of the back spiro attack. In the case of Mo insertion is more favorable than an attack from the back, but still not competitive with a direct front attack. With activation barriers that are calculated at least 5.3 kcal/mol (**1A** Cr) higher than for the direct front spiro attack, insertion can be ruled out in general. Moreover, precoordination of the olefin to the metal center was proposed as a necessary first step of the epoxidation reaction,[6,14] but we were unable to detect such a reaction

(41) Westland, A. D.; Haque, F.; Bouchard, J.-M. *Inorg. Chem.* **1980**, *19*, 2255−2259.

intermediate during our search of the potential energy surface. Recall that also for the structurally similar Re systems the insertion mechanism was ruled out due to unfavorable calculated reaction barriers.[12] A careful comparison[42] with the experimental activation barrier of the epoxidation of 4-methoxystyrene by the Re bisperoxo complex shows[39] that the calculated barriers underestimate experimental values by a few kcal/mol, in line with the general experience from density functional calculations.[23]

In the following we will focus on the direct front spiro attack as the most favorable reaction mechanism. There are three important observations (Table 4):

(a) The activation barriers for complexes of analogous structure decrease along the series Cr > Mo >W. The activation barriers of the W bisperoxo species **2A** and **2B** (10.7 and 16.9 kcal/mol, respectively) are quite close to the values calculated at the same computational level for structurally similar complexes $H_3CReO(O_2)_2$ and $H_3C(H_2O)ReO(O_2)_2$, 12.4 and 16.2 kcal/mol, respectively.[12]

(b) The barriers for the bisperoxo species are lower than those for the corresponding monoperoxo species; an especially large change of the activation barriers is computed for the coordinatively saturated complexes **1B** and **2B**.

(c) Coordination of a second base ligand to the monocoordinated species **1A** and **2A** significantly increases the activation barrier (cf. **1A** and **1B** as well as **2A** and **2B**).

The calculated structures of the transition states for the direct mechanism (Tables 2 and 3) exhibit a number of common features; in general, they resemble the structures of the transition states for direct oxygen transfer by Re and Ti peroxo complexes.[12,24,25] In the transition state, the structure of the ethylene moiety is only slightly distorted from the gas phase; e.g., the C−C distance elongated by at most 0.05 Å from the calculated gas-phase value of 1.33 Å. Thus, those values are significantly shorter than the C−C distance of ethylene oxide, which is calculated to 1.47 Å. Most of these transition states represent a synchronous approach of ethylene to the peroxo group with almost equal distances from the attacked oxygen center to each of the two carbon atoms. Relatively large differences of about 0.4−0.5 Å between O−C1 and O−C2 distances are computed for the attack of the front-side oxygen center of complex **1B** W and of the "back-side" oxygen center of the tungsten complexes **2A** and **2B** (Table 2). In these cases the ethylene molecule approaches the peroxo group in the vicinity of the equatorial NH_3 ligand and the corresponding sterical repulsion seems to be the reason for the asynchronous character of the transition state. Note that such asynchronous transition states correspond to rather high activation barriers (Table 4). In all transition structures the distance between the attacked oxygen atom and the metal center is only slightly stretched, by 0.05−0.1 Å, with respect to the value of the starting complex; the other M−O bond contracts concomitantly by about 0.1 Å. On the way to the transition state, the most important changes occur in the peroxo group: in the transition state the O−O distance is by 0.3−0.4 Å longer than in the reference intermediate. Although the O−O distances of the intermediates cover a moderately wide range, from 1.40 to 1.48 Å, depending on the metal center, the elongation of the peroxo bond in the transition state is rather uniform, 0.34−0.35 Å, for the complexes **2A** of Cr, Mo, and W (Table 2).

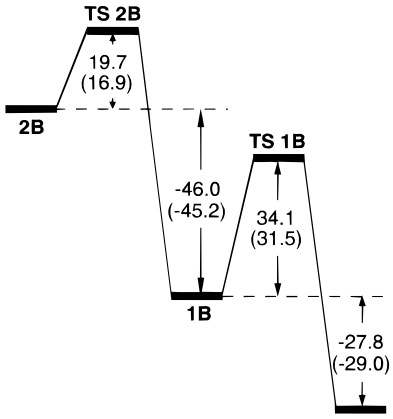

Figure 3. Energy profile of the epoxidation of ethylene by the peroxo complexes **2B** and **1B** of Mo and W. The activation barriers and reaction energies are given in kcal/mol; values are for W complexes.

It is also worth noting that the calculated structures of the synchronous transition states involving transition metal peroxo complexes are very similar to the transition state structures for the epoxidation of ethylene by dioxiranes studied also at the B3LYP level.[3]

Reaction Energies. In Figure 3 we characterize the reaction paths for ethylene epoxidation starting from the dicoordinated species **2B** of Mo and W. (The energy of the initial reagents, complex **2B** and two "free" ethylene molecules, is taken as reference.) After transfer of an oxygen atom from **2B** species **1B** is formed, which in turn can react with another ethylene molecule. The final products are the trioxo complex $(NH_3)_2M(O)_3$ and two molecules of ethylene oxide. In all cases, the transfer of an oxygen atom from the metal peroxo group is exothermic. However, there is a considerable difference between bisperoxo and monoperoxo complexes: for both Mo and W the monoperoxo complexes exhibit much smaller reaction energies, −27.8 and −29.0 kcal/mol, respectively, than the corresponding bisperoxo complexes, which feature barriers of −46.0 and −45.2 kcal/mol, respectively.

Discussion

Now, we turn to a discussion of the factors that govern the activity of transition metal peroxo complexes in olefin epoxidation. First, we address the mechanism of oxygen transfer from a metal peroxo group to the olefin substrate in general. Then we discuss in more detail the specific role of the metal center in activating or deactivating the peroxo group.

Electrophilic Character of Oxygen Transfer. Very many studies, both experimental and theoretical, have been devoted to epoxidation by purely organic oxidants such as peroxy acids and dioxiranes.[1−3,43−46] On the basis

(42) Rösch, N.; Gisdakis, P.; Yudanov, I. V.; Di Valentin, C. In *Peroxide Chemistry: Mechanistic and Preparative Aspects of Oxygen Transfer*; Adam, W., Ed.; Wiley-VCH: Weinheim, 2000.

(43) Hoveya, A. H.; Evans, D. A.; Fu, G. C. *Chem. Rev.* **1993**, *93*, 1307−1370.

(44) Adam, W.; Hadjiarapoglou, L. *Topics Curr. Chem.* **1993**, *164*, 46−52.

(45) Curci, R.; Dinoi, A.; Rubino, M. F. *Pure Appl. Chem.* **1995**, *67*, 811−822 and references therein.

(46) Koerner, T.; Slebocka-Tilk, H.; Brown, R. S. *J. Org. Chem.* **1999**, *64*, 196−201.

of these investigations, this reaction is described as an S_N2-like process in which a nucleophilic alkene is attacked by an electrophilic peroxy acid or dioxirane. In fact, the rate of epoxidation by these reagents is not very sensitive to steric hindrance, but is sensitive to electronic change: increasing the electron density of the alkene or decreasing that of the peracid increases the reaction rate. Also Hammett ρ values support this mechanism;[45,47−49] negative ρ values were obtained for the epoxidation of alkenes with both *m*-chloroperbenzoic acid and dimethyldioxirane while a positive ρ value was consistently observed for the epoxidation of *trans*-stilbene with substituted perbenzoic acids. Computational data confirmed the electrophilicity of the oxygen transfer by disclosing a partial electron density shift in the transition structures from olefin to peroxy acid or dioxirane (∼0.3 e).[2,3]

Olefin epoxidation by d^0 metal peroxo complexes closely resembles epoxidation by purely organic oxidants. This provides support for the conclusion that oxygen transfer by metal catalyzed reactions is also of electrophilic nature.[6,7] For example, peroxo and alkylperoxo complexes of transition metals react faster with electron-rich (highly alkyl substituted) olefins. The similarity of the electrophilic properties of $H_3C(H_2O)ReO(O_2)_2$ and dimethyldioxirane was demonstrated by the very similar ρ values obtained for the two oxidants in the reaction with styrene, $\rho = -0.92$ and -0.90, respectively.[49] Moreover, sulfoxidation of thiantrene 5-oxide, previously used as a mechanistic probe of the electrophilic character of dimethyldioxirane in oxygen transfer,[50] convincingly demonstrated the electrophilic nature of the peroxo oxygen centers in V, Mo, and W peroxo compounds: the oxygen atom is transferred from the peroxo complex to the electron-rich sulfide group of thiantrene 5-oxide rather than to the electron-poor sulfoxide group.[51] Computational results also corroborate the electrophilic nature of oxygen transfer from a metal peroxo complex to the olefin substrate in an epoxidation reaction. For the complex $H_3CReO(O_2)_2$ a decrease of the activation barrier was calculated when going from ethylene as substrate (12.4 kcal/mol) to its methyl-substituted derivatives; the lowest barrier, 6.3 kcal/mol, is computed for epoxidation of the fully substituted tetramethylethylene.[24]

Frontier Orbital Interaction. As in preceding studies,[12,24,25] the electrophilic character of the oxygen transfer is manifested through the electron density transfer in the transition state, about 0.2 e, from ethylene to the peroxo complex. In terms of the molecular orbital structure, such transfer results from the interaction of the π(C−C) HOMO of ethylene and the unoccupied O−O antibonding orbital σ*(O−O) (Figure 4) of the peroxo complex; this interaction leads to a breaking of the O−O bond of the peroxo group.[24] Note that the σ*(O−O) level is not the LUMO of the complexes, but lies slightly above the manifold of vacant d-levels of the metal center. However, the spatial structure of the σ*(O−O) orbital allows a significant overlap with the olefin orbitals, different from the rather localized vacant d-orbitals of the metal center.

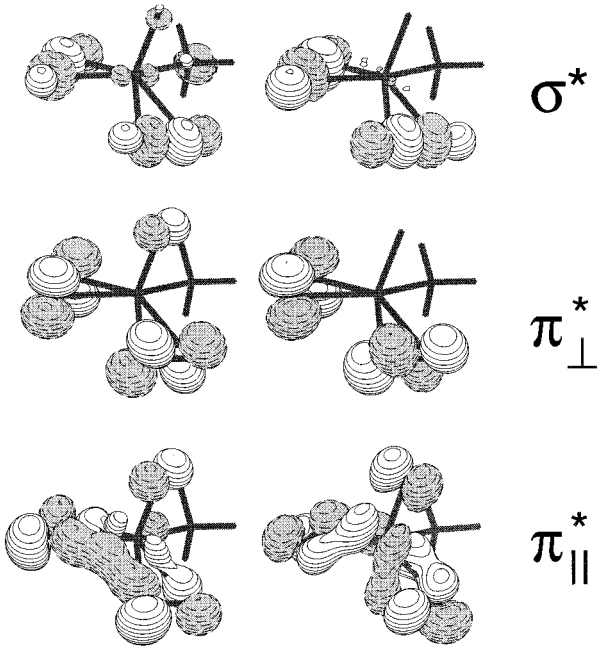

Figure 4. Molecular orbitals of the model complex W **2A** near the HOMO−LUMO gap with dominant contributions of the peroxo groups.

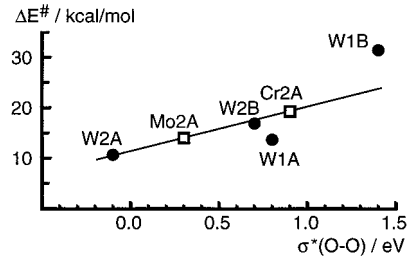

Figure 5. Calculated activation energies $\Delta E^{\ddagger}$ as function of the σ*(O−O) orbital energies (averaged value in case of **2A** and **2B**). The linear regression line is derived from the three points that correspond to the data of the model complexes **2A**.

The energy of the unoccupied antibonding σ*(O−O) level plays an important role in determining the activity of the peroxo complex in oxygen transfer,[24] since it reflects the ability of the peroxo group to accept additional electron density from the olefin HOMO. In a previous study of Re and Ti peroxo complexes we have established a linear correlation between the energy of the σ*(O−O) orbital of the complex and the height of the activation barrier: for a fixed electron donor, the higher the energy of the σ*(O−O) level, the higher the activation barrier.[24,25] In Figure 5 the calculated activation energies of ethylene epoxidation (front spiro attack) are plotted against the energies of the σ*(O−O) level of the corresponding intermediates. One deduces that the complexes considered in the present study also comply with such a linear trend between barrier height and energy of the acceptor σ*(O−O) orbital.

Atomic Charges. It is natural to use the calculated atomic charges as a criterion of the electrophilic character of the peroxo group. There is some correlation between the charge of the oxygen center to be transferred and the corresponding activation barrier when different complexes of the same metal are considered (Table 2). For instance, the oxygen center O2 at the "back-side" (Figure 1) always exhibits a larger negative charge, by 0.04 to

(47) Hanzlik, R. P.; Shearer, G. O. *J. Am. Chem. Soc.* **1975**, *97*, 5231−5233.
(48) Dryuk, V. G. *Tetrahedron* **1976**, *32*, 2855−2866.
(49) Al-Ajlouni, A. M.; Espenson, J. H. *J. Org. Chem.* **1996**, *61*, 3969−3976.
(50) (a) Adam, W.; Golsch, D. *Chem. Ber.* **1994**, *127*, 1111−1113. (b)
(51) Adam, W.; Golsch, D.; Sundermeyer, J.; Wahl, G. *Chem. Ber.* **1996**, *129*, 1177−1182.

0.07 e, than the "front-side" oxygen center O1; concomitantly the activation barrier for back attack is always significantly higher than that for a front attack (Table 4). The reason for the structural asymmetry of the metal-peroxo group and concomitant charge distribution can be related to orbital overlap. A rotation by 20−25° from the symmetric position, around an axis through the metal center perpendicular to the M−O−O plane, yields optimal overlap between metal d and ligand orbitals. Thus, such a structural deviation from an ideal symmetric structure helps to maximize the interaction between the peroxo π system and the two metal d orbitals which determine the M−O peroxo bonds (see Figure 4).

However, since the charges of peroxooxygen centers of complexes with the same metal center vary only little, by at most 0.1 e (Table 2), steric repulsion from the neighboring base ligand (besides electronic effects) might also contribute to the higher activation barriers of the back attack.

The same type of complexes (**2A**; see Table 3), but of different transition metals, exhibits a clear trend of the negative NBO atomic charge of the oxygen centers: they increase along the series Cr (−0.23 e), Mo (−0.38 e), W (−0.44 e). However, this trend is at variance with the decrease of the activation barrier of oxygen transfer calculated for the same series of complexes, from 19.3 to 14.1 to 10.7 kcal/mol (front spiro attack, Table 4). To resolve this contradiction we consider next in more detail the relationship between the occupation of the orbitals of the peroxo moiety and the strength of O−O bond.

Strength of the O−O Bond in the Peroxo Group. The analysis of the calculated transition state structures shows that O−O bond activation is a discriminating factor for the reactivity of peroxo complex: the O−O bond is significantly elongated compared to the reactive intermediate, while the distance between metal center and attacked oxygen is hardly changed. As already pointed out, the length of the O−O bond is a typical characteristic of complexes of a given metal center and it hardly varies when the coordination shell of complex (e.g. the number of peroxo groups or base ligands) changes. In complexes **2A** the length of O−O bond increases from 1.40 Å for Cr to 1.45 and 1.48 Å for Mo and W, respectively (Table 2), in line with the decrease of the calculated activation barrier as just noted. As far as the O−O distance can serve as an indicator of the O−O bond strength, it provides a rationale for the trend of the calculated activation barriers: they are the lower, the longer the O−O distance is.

It is instructive to compare the calculated O−O distances of metal complexes with the corresponding value of an isolated H_2O_2 molecule. In the W complexes the peroxo bond is by about 0.03 Å longer than in hydrogen peroxide (1.45 Å, calculated at the same level). This finding indicates an activation of the peroxo group by the metal center. The O−O distances in the Mo complexes are very close to the value of H_2O_2 while for Cr complexes the O−O distance is calculated noticeably shorter than H_2O_2, by about 0.05 Å, indicative of a deactivation of the peroxo group and in line with the value of the calculated barrier for oxygen transfer (cf. Table 3).

Orbital Interaction between the Metal Center and the Peroxo Ligand. To elucidate the mechanism of activation or deactivation of the peroxo group by the metal center, one has to analyze the M−O interaction that is also responsible for the distribution of charge between the metal center and peroxo group. A peroxo group, formally an O_2^{2-} ligand, interacts with the metal center via donation from its filled orbitals to the formally empty d orbitals of metal center. The highest occupied orbitals of peroxo ligand are the O−O antibonding orbitals $\pi_\perp$*(O−O) and $\pi_{||}$*(O−O) (see Figure 4); the $\pi_\perp$* orbital has a node in the plane M−O−O. In the bisperoxo complexes, each of these levels splits into a pair of nearly degenerate orbitals, one symmetric and the other antisymmetric with respect to the plane O=M−N (Figure 4). These highest occupied orbitals are stronger involved in the interaction with d orbitals of metal center than the lower lying O−O bonding levels $\pi_\perp$, $\pi_{||}$, and σ.[25] Involvement of metal d orbitals reduces the O−O antibonding character of the π* orbitals and thus leads to a strengthening of the O−O bond. Simultaneously, the charge of the peroxo oxygen centers decreases. Thus, the metal peroxo interaction determines two competitive factors that influence the epoxidation activity: the electrophilicity of the oxygen centers and the strength of O−O bond.

It is important to understand how these interactions between the metal center and the peroxo groups vary for different metal centers. Based on the following arguments we will rationalize the calculated elongation of the O−O bonds in the series of Cr, Mo, W peroxo complexes as a consequence of the weakening of the interaction between the π*(O−O) and d(M) orbitals.

(a) Energy and radial extension of the d(M) orbitals increase along the triad from the first to the third row, but they are rather similar for Mo and W due to the "lanthanide contraction". Therefore, Cr exhibits the lowest lying d orbitals[52] available for donation from π*(O−O) orbitals.

(b) The polarizing power of a metal cation, which determines the covalent character of the ligand bonds, varies inversely with its ionic radius. Thus, for Cr we observe the smallest charge separation in the M−O bond which indicates the highest electron density in vicinity of the metal center or, in other words, the largest donation from π*(O−O). The NBO analysis corroborates this argument. With positive net charges at the metal center of 0.93, 1.96 and 2.24 e in the complexes **2A** of Cr, Mo, and W, respectively, (Table 3) it yields a higher electron population at the Cr center than at Mo and W centers. The net negative charges of the peroxo oxygen centers increase concomitantly, from −0.23 to −0.38 and −0.44 e for O1 in **2A** species of Cr, Mo, and W, respectively. The NBO analysis also yields contributions of the metal center to the metal-peroxo bond which decrease along Cr (25%) > Mo (17%) > W (15%); see Table 3.

(c) The stability of the highest oxidation state increases in the series Cr, Mo, W. Cr(VI) is in fact a strong oxidizing agent and therefore a very good electron acceptor.[53] To illustrate this statement we calculated the energy difference between the closed-shell ground state of the complexes **2A** to the lowest-lying triplet state. This excitation corresponds to a formal transfer of an electron from a peroxo ligand to the d manifold of the metal center or, in other words, to a formal reduction of the metal center to M(V) and the formation of a superoxide ligand. In fact, the optimized O−O distance of about 1.30 Å in

(52) Neuhaus, A.; Veldkamp, A.; Frenking G. *Inorg. Chem*. **1994**, *33*, 5278−5286.

(53) Lee, J. D. In *Concise Inorganic Chemistry;* Chapman & Hall: London, 1991; pp 713−722.

the triplet states of the complexes of all three elements is typical for a superoxide. Most importantly, the vertical excitation energy increases from 1.0 eV for the Cr complex to 3.0 and 3.7 eV for Mo and W, respectively.

In summary, a strong donation from the occupied antibonding levels of the peroxo group of the Cr complex deactivates the peroxo bond, although the oxygen centers of these species are formally less negative than those of the corresponding Mo and W complexes. Clearly, the calculated trends in the series Cr, Mo, W cannot be rationalized from the charge distribution alone; rather, it is crucial to also invoke the underlying orbital interactions.

Base Effect. The introduction of a second base ligand, NH_3, into the monocoordinated species **1A** and **2A** leads to a significant increase of the activation barrier as calculated for species **1B** and **2B**, respectively (Table 4). The electronic effect of the base ligands (in particular, of a second ligand which significantly increases the activation barrier) has been already discussed in terms of orbital interactions for the example of Ti peroxo complexes.[25] This inhibiting effect of the base ligands is common for all transition metal peroxo complexes so far studied computationally; analogous trends of increased activation energies concomitant with an increased number of base ligands have been obtained in calculations of Re mono- and bis-peroxo complexes.[12,24] A joint experimental and theoretical study[24] on different base adducts of the bis-peroxo complex $(H_3C)ReO(O_2)_2$ revealed that coordination of a base to the complex induces, mediated via the metal center, additional electron density on the peroxo group. This, in turn, pushes the antibonding "acceptor" level $\sigma^*(O-O)$ upward and results in a higher activation barrier.[24,25]

A similar picture is obtained for the complexes of the present study. The $\sigma^*(O-O)$ level shifts to higher energies (Figure 5) and the charge of the oxygen centers increases for the dicoordinated species **1B** and **2B** compared to monocoordinated **1A** and **2A**, respectively. However, the large increase of the activation barriers of the monoperoxo complexes **1B** compared to **1A** (Table 3) cannot be traced to the rather small changes in the calculated characteristics of the peroxo group. In particular, the charge of the "front-side" oxygen center, O1, increases only by 0.03 e when going from the complex **1A** of W to the corresponding complex **1B** (Table 2). This provides evidence for the plausible assumption that a repulsive interaction between the NH_3 ligand and the ethylene substrate also affects the activation in **1B**. Further support for this viewpoint is obtained from the asynchronous approach of ethylene to the peroxo group in this case; in the epoxidation transition state starting from **1B** W the distances O1−C1 and O1−C2 are 1.81 and 2.17 Å, respectively (Table 2).

Monoperoxo vs Bisperoxo Complexes. The high activation barriers calculated for the monoperoxo species **1A** and **1B** may, to some extent, also be attributed to the higher negative charge of the oxygen centers of these complexes compared to those of the corresponding bisperoxo species **2A** and **2B** (Table 2). In this context is seems helpful to refer to a more detailed discussion of all factors governing the activity of Mo monoperoxo complexes where different types of anionic ligands formally replace one of the peroxo groups of the bisperoxo complex.[54]

Conclusions

Using B3LYP hybrid density functional calculations, we have studied the epoxidation of ethylene as model olefin by oxo-bisperoxo and dioxo-monoperoxo complexes of Cr(VI), Mo(VI), and W(VI). The calculations reveal that the epoxidation reaction proceeds preferentially as direct attack of the nucleophilic olefin on an electrophilic peroxo oxygen center via a transition state of spiro structure. For the insertion mechanism much higher activation barriers were obtained. For a series of structurally identical complexes the calculated activation barriers of direct oxygen transfer to ethylene decrease along Cr > Mo > W with W complexes being the most active. These computational results are in line with the experimentally reported higher activity of W species compared to Mo.[15] The calculated low activity of the Cr peroxo complexes was rationalized by the deactivating effect of the Cr(VI) center that withdraws electron density from the antibonding π^* levels of peroxo group and thus strengthens the O−O bond. The activation barrier of about 17 kcal/mol calculated for the 7-coordinated W bisperoxo complex is close to the values calculated at the same level for structurally similar Re complexes, 13−16 kcal/mol,[12,24] which in turn have been found lower than experimental values by a few kcal/mol.[39]

The calculated barriers for the oxo-bisperoxo species are lower than those for the corresponding dioxo-monoperoxo species; the epoxidation reactions of the latter complexes are also calculated to be less exothermic. Coordination of a second NH_3 base ligand to the low-coordinated species $(NH_3)M(O)_2(O_2)$ and $(NH_3)MO(O_2)_2$ significantly increases the activation barrier and deactivates the complex. This finding agrees with the experimentally known low activity of Mo and W peroxo complexes in strongly coordinating solvents.[14,20,21] The main reason for this effect is induction of additional electron density from the base ligand to the peroxo group, mediated via the metal center. This reduces the electrophilicity of the peroxo group and pushes the antibonding $\sigma^*(O-O)$ level upward, resulting in a higher activation barrier.

In a series of density functional studies on the mechanism of olefin epoxidation by the transition metal peroxo compounds we have considered various factors that govern the activity of the peroxo group, like the effect of base and anionic ligands, competition between peroxo and hydroperoxo (or alkylperoxo) groups.[12,24,25,42,54] The present work complements this series of studies by elucidating the strong influence of the metal center on the epoxidation activity of an η^2-coordinated peroxo group. This effect can be activating as in the case of W or deactivating as in the case of Cr.

Acknowledgment. We thank P. Hofmann, H. Rothfuss, and J. H. Teles for helpful discussions. This work was supported by the Deutsche Forschungsgemeinschaft, the German Bundesministerium für Bildung, Wissenschaft, Forschung und Technologie (grant no. 03D0050B), INTAS-RFBR (IR-97-1071), and the Fonds der Chemischen Industrie.

JO9916784

(54) Yudanov, I. V.; Di Valentin, C.; Gisdakis, P.; Rösch, N. *J. Mol Catal. A* **2000**, in press.